Terahertz Signatures of Hydrate Formation in Alkali Halide Solutions

Ligang Chen,[†,¶] Guanhua Ren,[†,¶] Liyuan Liu,[†,*] Pan Guo,[‡] Endong Wang,[‡] Lu Zhou,[†] Zhongjie Zhu,[‡] Jianbing Zhang,[¶,‡] Bin Yang,[§] Wentao Zhang,[ᵟ] Yanfeng Li,[†] Weili Zhang,[†,⊥] Yi Gao, [¶,‡] Hongwei Zhao,[¶,‡,*] and Jiaguang Han[†,*]

[†] Center for Terahertz Waves and College of Precision Instrument and Optoelectronics Engineering, Tianjin University, Tianjin 300072, People's Republic of China

[¶] Shanghai Advanced Research Institute Zhangjiang Lab, Chinese Academy of Sciences, Shanghai 201210, China

[‡] Division of Interfacial Water and Key Laboratory of Interfacial Physics and Technology, Shanghai Institute of Applied Physics, Chinese Academy of Sciences, Shanghai 201800, China

[§] Faculty of Science and Engineering, University of Chester, Thornton Science Park, Chester, U.K. CH2 4NU

[ᵟ] Guangxi Key Laboratory of Optoelectronic Information Processing, Guilin University of Electronic Technology, Guilin 541004, China

[⊥] School of Electrical and Computer Engineering, Oklahoma State University, Stillwater, Oklahoma 74078, United States

Corresponding Authors:
*lyliuma@tju.edu.cn
*zhaohongwei@sinap.ac.cn
*jiaghan@tju.edu.cn

ABSTRACT: We systematically studied the ability of 20 alkali halides to form solid hydrates in the frozen state from their aqueous solutions by terahertz time-domain spectroscopy combined with density functional theory (DFT) calculations. We experimentally observed the rise of new terahertz absorption peaks in the spectral range of 0.3-3.5 THz in frozen alkali halide solutions. The DFT calculations prove that the rise of observed new peaks in solutions containing Li^+, Na^+ or F^- ions indicates the formation of salt hydrates, while that in other alkali halide solutions is caused by the splitting phonon modes of the imperfectly crystallized salts in ice. As a simple empirical rule, the correlation between the terahertz signatures and the ability of 20 alkali halides to form a hydrate has been established.

TOC GRAPHICS:

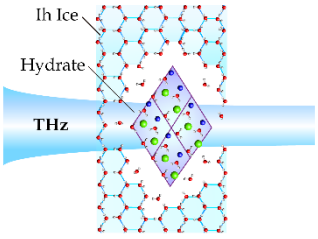

LiF	LiCl	LiBr	LiI
NaF	NaCl	NaBr	NaI
KF	KCl	KBr	KI
RbF	RbCl	RbBr	RbI
CsF	CsCl	CsBr	CsI

The formation of salt hydrates is important in understanding diverse phenomena in chemistry and also is critical to many practical applications in geology, climatology and pharmacy. In geology, the identification of hydrates that are ubiquitous in glacier minerals such as hydrohalite can improve the understanding of diagenesis.[1-3] In astronomy, salt hydrates within saline deposits on Mars and Europa were found to be evidence of the presence of water.[4-6] In climatology, hydrated salts have been proven to be better nuclei for cloud formation than nonhydrated salt particles.[7,8] More generally, the nature of salt hydrates has widespread significance in the fields of biology and food science, such as cell survival under freeze-thawing[9] and low-temperature preservation of biological tissues and foods.[10,11]

Studies of salt hydrates conducted thus far include a number of different techniques, such as nuclear magnetic resonance (NMR),[12,13] X-ray diffraction (XRD)[14-17] and neutron diffraction,[18-20] where the crystal structures, the structural environments and the ratio of ions and water molecules of the salt hydrates can be evaluated. Infrared (IR) spectroscopy has also been widely utilized for investigations of hydrate formation in various aqueous salt solutions by cooling.[21-28] As it provides sensitivity to the high frequency O-H vibrational information, IR spectroscopy could be a useful tool in the characterization of structural changes during hydrate

formation.[21-24,29] With the recent advent of a new spectroscopic technique, terahertz time-domain spectroscopy (THz-TDS), the far-infrared lower frequency properties of materials in the range below 3.5 THz can be readily obtained.[30-32] Unlike IR spectroscopy, terahertz spectra are more sensitive to molecular conformational and structural changes.[31,33] In 2018, Ajito and coauthors captured the appearance of new terahertz absorption peaks at around 1.5-1.6 and 2.3-2.4 THz during the formation process of NaCl hydrates and these peaks were assigned to the intermediate of NaCl hydrates.[34] Our recent work also reported the observation of NaCl hydrate formation in aqueous solution and the preliminary results indicated that the formed NaCl hydrate produces new terahertz absorption peaks at around 1.6, 2.43, 3.34, and 3.78 THz.[35] Here we systematically study the hydrate formation of 20 alkali halides from their aqueous solutions in the frozen state by using THz-TDS and explore the correlation of terahertz signatures with their ability to form hydrates.

In figures 1a-1e, the terahertz spectra of water and the first series of four chloride salt tablets (NaCl, KCl, RbCl, and CsCl) recorded at room temperature are shown by the dotted blue lines, and the corresponding spectra of their frozen aqueous solutions at 223 K are presented by the solid red lines. No remarkable terahertz absorption peaks are observed for either the liquid water or the ice over the frequency range of 0.3-3.5 THz, whereas the ice is more transparent than the liquid water due to the constrained thermal fluctuation of the hydrogen bonds. The low, smooth terahertz absorption of the ice is an ideal background for studying hydrate formation processes. Figure 1b illustrates the terahertz spectra of the solid NaCl tablet and the frozen aqueous NaCl solution. Compared with the terahertz spectrum of the solid NaCl tablet, new terahertz absorption peaks are observed at 1.60, 2.43, and 3.34 THz in the aqueous NaCl solution in the frozen state. Since these absorption peaks do not exist in the terahertz spectra of either the ice or the solid NaCl tablet, they arise entirely from the newly formed frozen structures. The direct evidence comes from the XRD measurements. A low-temperature (223 K) XRD experiment was implemented with the 1 mol/L NaCl solution, and the diffraction patterns are presented as orange lines in Figure 1g. Compared with ice (Ih ice PDF: 85-0857) and NaCl crystals (NaCl PDF: 70-2509), there are obvious new diffraction peaks in the frozen NaCl solution, as indicated by the purple arrows in Figure 1g. The assignments of the measured XRD patterns suggest the newly formed structure: $NaCl{\cdot}2H_2O$ hydrate ($NaCl{\cdot}2H_2O$ PDF: 70-1158). Hence, it is evident that the observed terahertz absorption peaks are caused by the formed $NaCl{\cdot}2H_2O$ hydrate, and the characterized peaks originate from collective vibrations of all molecules in the hydrate crystal.[35] The absorption peaks at 1.60 and 2.43 THz were also observed in frozen NaCl solution during the freeze-drying process. These two peaks were assigned to metastable unit-cell-sized distorted NaCl particles rather than the dihydrate $NaCl{\cdot}2H_2O$ crystals since $NaCl{\cdot}2H_2O$ has no dipole moment for inducing terahertz absorption peaks.[34] However, the terahertz peak can also be contributed by the lattice vibration of the non-dipole -moment crystal. As discussed in ref. 35, these two peaks, together with the peak at 3.34 THz, were assigned ideally to the specific vibration forms of a hydrate crystal by DFT.

Now for the other salts in this series, i.e., KCl, RbCl, and CsCl, Figures 1c-e shows their measured terahertz spectra. It can be seen that all of the frozen aqueous KCl, RbCl, and CsCl solution samples display absorption profiles similar to those

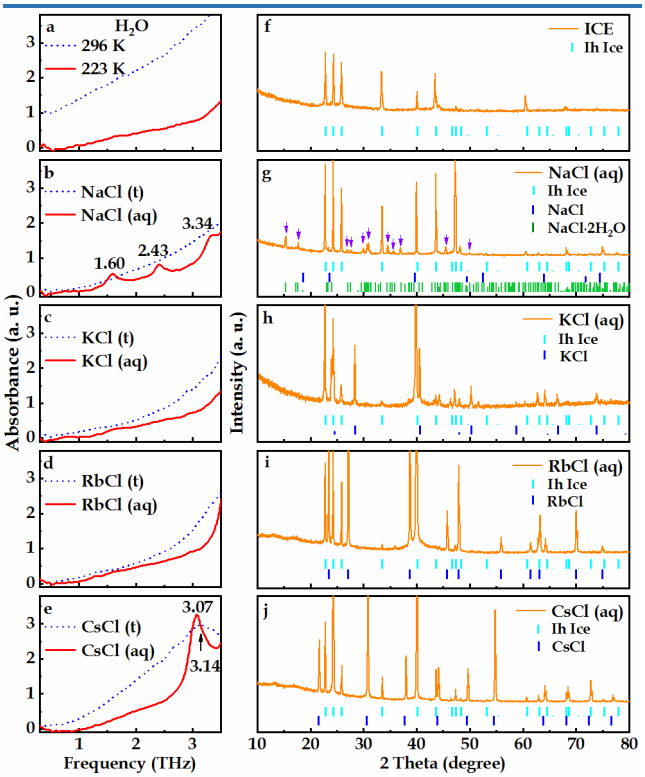

Figure 1. (a) Terahertz spectra of water measured at 296 K (dotted blue line) and 223 K (solid red line). (b-e) Terahertz spectra of four alkali chloride tablets (t, dotted blue lines) measured at 296 K and their 1 mol/L solutions (aq, continuous red lines) measured at 223 K (frozen state). (f-j) Corresponding XRD results of the frozen alkali chloride solutions (orange lines), where the vertical lines below the XRD patterns indicate the positions of diffraction from hexagonal ice (H_2O Ih, cyan lines), salts tablets (blue lines), and $NaCl{\cdot}2H_2O$ crystals (green lines).

observed in their corresponding tablet samples. Unlike the case of NaCl, no additional terahertz absorption peaks are observed in the spectra below 3.5 THz in frozen aqueous KCl and RbCl solutions. This can be further confirmed by the XRD patterns illustrated in Figure 1h-i, where the diffraction peaks of the frozen aqueous salt solutions agree well with the superposed diffraction peaks of the ice and the salt crystal. The assignments of the measured XRD patterns clearly indicate that there is no new hydrated structure formed during freezing the aqueous KCl and RbCl solutions. One may notice that in CsCl solution a sharp peak at 3.07 THz appears in the frozen sample at 223 K. The appearance of this peak might be caused by two possible reasons. First, the formed hydrates produce the new absorption peaks, similar to that in the NaCl solution. Second, temperature and geometry effects in frozen solution give rise to the narrowed and red-shifted band at 3.07 THz compared with that of the CsCl tablet at 3.14 THz.[36,37] The terahertz absorption peaks of both the CsCl tablet and frozen CsCl solution originate from lattice vibrations of the cubic crystal.[38] Comparing the XRD patterns of the frozen CsCl solution with those of the CsCl tablet and the ice shown in Figure 1j, we found that the diffraction peaks of the frozen aqueous CsCl solutions agree well with the superposed diffraction peaks of the ice and the CsCl tablet. Hence, there are no new hydrated structures formed in the aqueous CsCl solutions upon freezing.

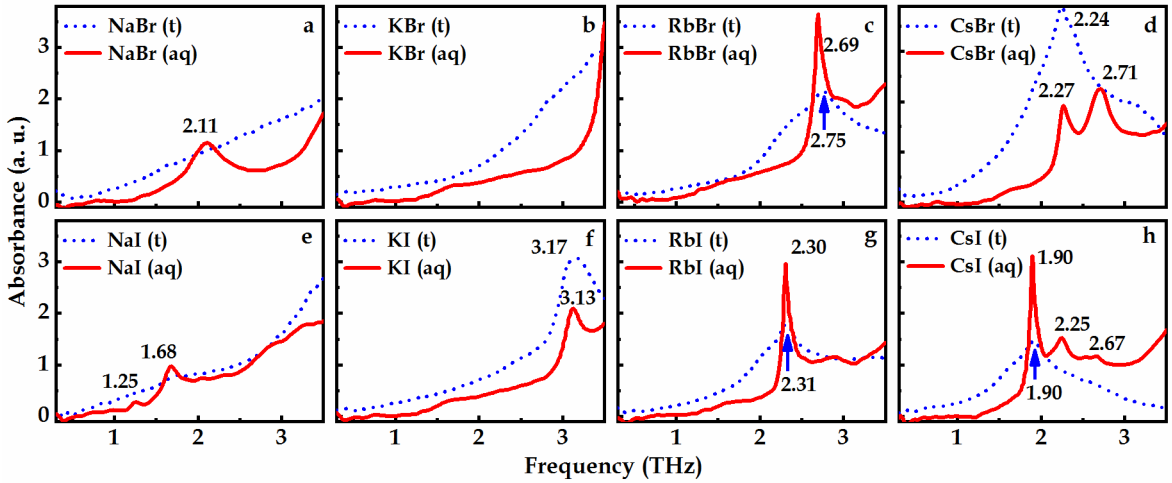

Figure 2. Terahertz spectra of solid salt powders at room temperature (dotted blue lines) and 1 mol/L salt solutions at 223 K (solid red lines).

Thus far, the terahertz studies of the first series of chloride salts have shown that the significant change in the terahertz spectrum with the emergence of discrete peaks provides visible indications of the salt hydrate formation. The result also implies that the sodium ion has a substantial effect on the salt hydrate formation compared to the other alkali ions K^+, Rb^+, and Cs^+. To investigate the effects of different ions on the hydrate formation, we performed experiments on the second series containing salts NaBr, NaI, KBr, KI, RbBr, RbI, CsBr, and CsI.

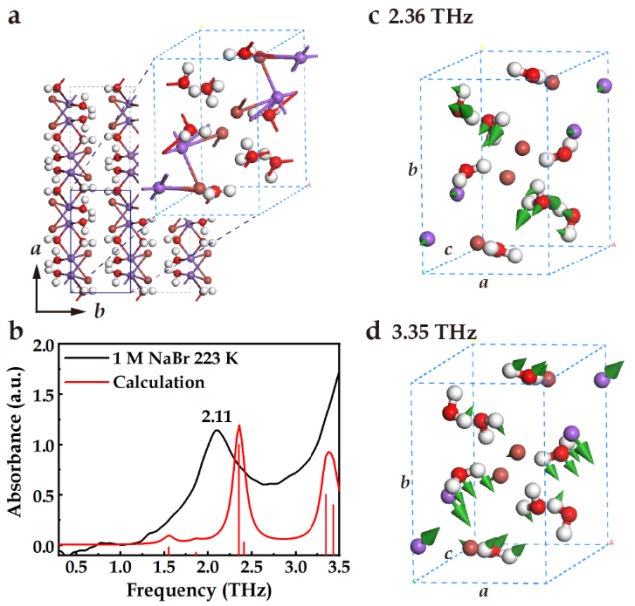

Figure 3. Theoretical calculation results of terahertz spectroscopy and the corresponded vibrational modes of $NaBr{\cdot}2H_2O$. (a) Crystal structure of $NaBr{\cdot}2H_2O$ viewed along the *c* axis, with the enlarged frame showing a unit cell. The periodic boundary condition is employed in the calculation. The parameters of the unit cell are a = 6.570 Å, b = 10.380 Å, c = 6.780 Å, β = 113.5°, and $\alpha = \gamma$ = 90°.[39] Na^+ and Br^- are represented by purple and brown balls, respectively. (b) Experimental and calculated terahertz spectra of $NaBr{\cdot}2H_2O$. (c, d) Calculated vibrational modes of $NaBr{\cdot}2H_2O$ at (c) 2.36 THz and (d) 3.35 THz.

Figure 2 illustrates the measured terahertz spectra of the salts in this series.

By comparing the terahertz spectra of the frozen salt solutions at 223 K with those of the salt tablets at 296 K, it is obvious that there are new absorption peaks in frozen NaBr (at 2.11 THz) and NaI (at 1.25 and 1.68 THz). In our previous study of NaCl, the terahertz absorption peaks in frozen solution were assigned to vibrational modes of the $NaCl \cdot 2H_2O$ crystal[35]. Given this study, it can be speculated that the new terahertz observed peaks in frozen NaBr and NaI solutions are probably caused by the formation of dihydrates.[39,40] To verify this speculation, we performed density functional theory (DFT) calculations on $NaBr \cdot 2H_2O$. The results are plotted in Figure 3, and the used parameters from ref. 39 are listed in the caption. The vibrational mode at 2.36 THz, corresponding to the peak at 2.11 THz in the experimental spectra, arises from collective vibrations of all molecules in the unit cell, and mainly comes from the collective vibrations of water molecules along the long diagonal at an angle of about ± 45° with respect to the *ac* plane. The peak at 3.35 THz, corresponding to the experimental peak above 3.5 THz, can be assigned to the translational vibration of Na^+, and Br^- ions and parts of the water molecules along the short diagonal at an angle of about ± 45° with respect to the *ac* plane. The DFT calculation on $NaBr{\cdot}2H_2O$ confirms that the newly discovered terahertz absorption peaks in the frozen NaBr solution originate from the vibrational modes of the $NaBr{\cdot}2H_2O$ crystal. Similar to NaCl and NaBr solutions, other sodium halides also produce new terahertz absorption peaks in the frozen state. The terahertz features mainly originate from collective vibrations of molecules in hydrate crystals, and each feature has been marked as being part of a specific vibrational mode.

For CsBr and CsI solutions, there are also new absorption peaks observed in frozen solutions of CsBr (at 2.71 THz) and CsI (at 2.25 and 2.67 THz). The strongest absorption peaks match well with the peaks observed in their tablets, which originate from lattice vibrations of the anhydrous salt cubic crystal (as shown by dotted blue lines in Figure 2), while there are peaks observed at frequencies higher than the lattice vibrational mode. The appearance of new peaks might be

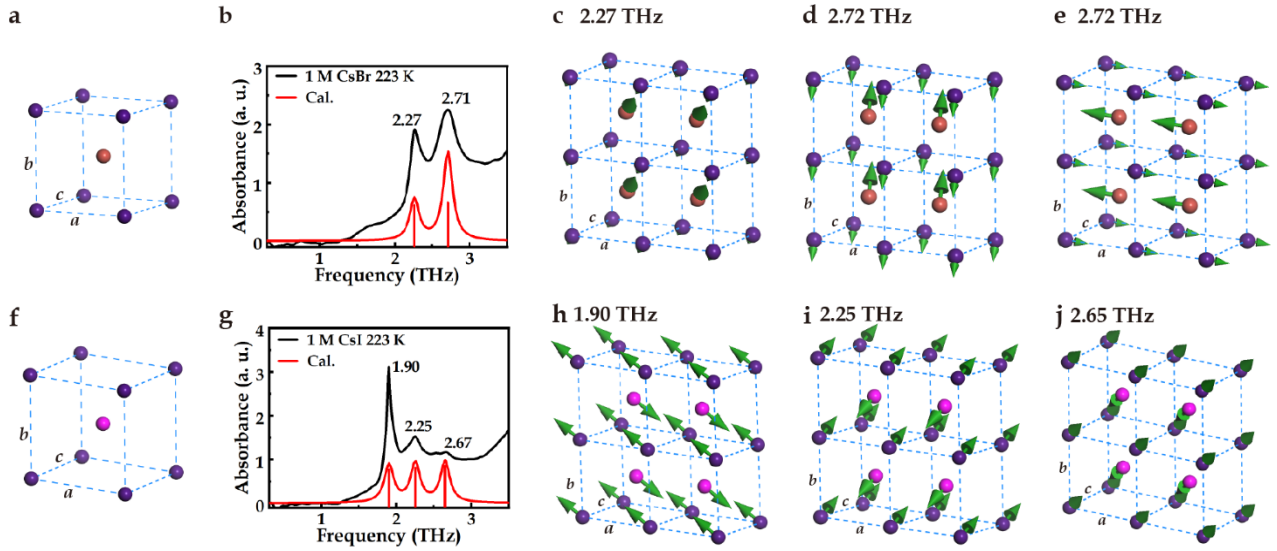

Figure 4. Theoretical calculation results of terahertz spectroscopy and the corresponding vibrational modes of (a-e) CsBr and (f-j) CsI. The crystal structures of CsBr and CsI, and periodic boundary condition are employed in the calculation. The parameters of the unit cell are (a) $a = b = c = 4.163$ Å, and $\alpha = \beta = \gamma = 88.7°$and (f) $a = b = c = 4.410$ Å, $\alpha = 90°$, $\beta = 91.7°$, and $\gamma = 93°$. Cs^+, $Br^-$and I^- are represented by purple-black, brown and pink balls, respectively. Experimental and calculated terahertz spectra of (b) CsBr and (g) CsI. Calculated vibrational modes of CsBr at (c) 2.27 THz and (d-e) 2.72 THz and of CsI at (h) 1.90 THz, (i) 2.25 THz, and (j) 2.65 THz.

caused by the formation of hydrates and/or the distortion of the nonhydrated crystals. However, Iglev's work in 2010 experimentally proved that CsBr and CsI salts do not form hydrates because of their high enthalpies of solution.[24] Thus, these newly generated peaks are due to the lattice vibration of distorted CsBr and CsI crystals restricted in the local environment of surrounding ice. Similar lattice distortion has already been observed for nanocrystals[41,42] and doped-crystals[43]. It is worth mentioning that in CsCl solution there is no phonon mode splitting observed in the frozen state. This is probably because of both the limitation of the available frequency region in the experiment and the instability of the tilted CsCl crystal compared with CsBr and CsI.

To theoretically investigate the origin of the freezing-induced peaks in these nonhydrated salts, we also performed DFT calculations, and the results of CsBr and CsI are plotted in Figure 4. For a distorted CsBr crystal with parameters of $a = b = c = 4.163$ Å and $\alpha = \beta = \gamma = 88.7°$, the features of the calculated spectra capture the terahertz experimental results well. The calculated vibrational mode at 2.27 THz matches the measured peak at 2.27 THz. This peak arises from the collective Cs^+ and Br^- ion vibrations in the short diagonal direction at an angle of about 45° to the *ac* plane (Figure 4c). The peak at 2.72 THz, corresponding to the experimental peak at 2.71 THz, is assigned to the same two energy vibrations lying in the short diagonal direction at an acute angle with respect to the *ac* plane (Figure 4d) and in the long diagonal direction at an acute angle with respect to the *ac* plane (Figure 4e).

Similarly, Figures 4f-j shows the theoretical calculation results of terahertz spectroscopy and the corresponding vibrational modes of the CsI imperfect crystal, and the parameters of the CsI crystal structure are $a = b = c = 4.410$ Å, $\alpha = 90°$, $\beta = 91.7°$, and $\gamma = 93°$. The calculation captured the terahertz experimental results weel. These absorption peaks

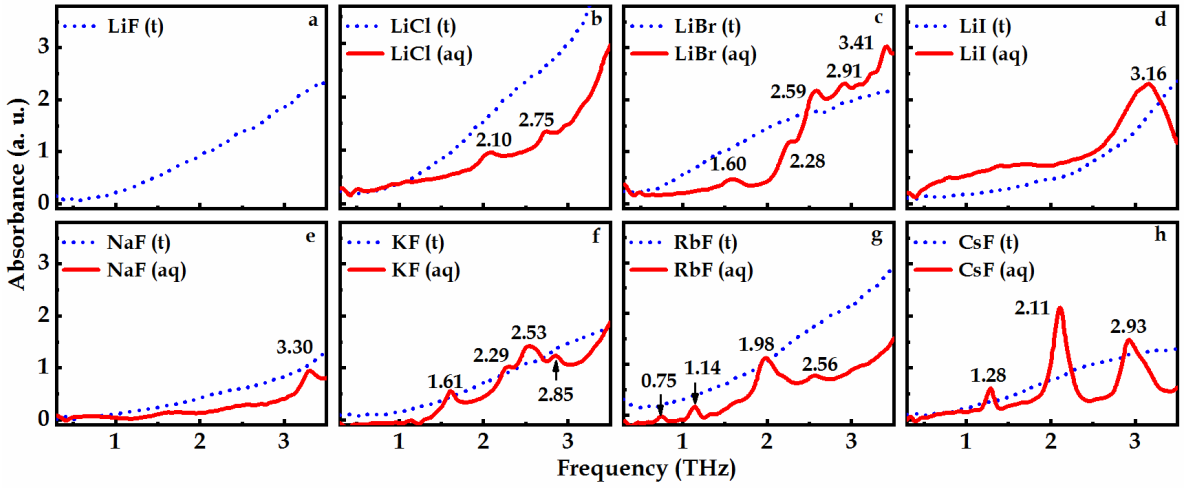

Figure 5. Terahertz spectra of lithium halides and alkali fluorides: the dotted blue lines and continuous red lines represent solid salts at room temperature and the frozen aqueous salts, respectively.

originate from the lattice vibration of a distorted CsI crystal with different energies in three vibrational directions. The good agreement between the calculated spectra terahertz of distorted nonhydrated crystals and the measured spectra of frozen solutions confirms that the newly discovered terahertz absorption peaks in the frozen CsBr and CsI solutions are derived from the lattice vibration of the imperfect crystals rather than the hydrate formation. These two salt solutions are prone to lattice distortion in the frozen state, which may be due to the large atomic radius of these ions making them easy to deform. These results also verify that the Br^- and I^- anions do not have a visible influence on the formation of salt hydrates, while alkali cation Na^+ still has important roles.

In addition to the above alkali halides, our study is carried out on the third series containing salts LiF, LiCl, LiBr, LiI, NaF, KF, RbF, and CsF. The influence of F^- and Li^+ ions on the salt hydrate formation is further investigated. Different from the salts in the first and second series, the lithium and fluoride salts show some specific features. Salt LiF has very poor water solubility. The unsaturated lithium salt solutions of LiCl, LiBr, and LiI, such as at 1 mol/L, are prone to supercooling in our freezing experiments even if the temperature drops to the limit of our equipment, 80 K. However, their saturated solutions are easy to nucleate and crystallize during the freezing process due to supersaturation. Similarly, the fluoride salt solutions of NaF and CsF at the saturated concentrations are also used in our experiment to avoid supercooling. The KF and RbF solutions are adopted at the same concentration of 1 mol/L as in the previous series. Figure 5 presents the terahertz spectra of the salt samples in the third series. Except for LiF, newly emerging peaks are observed in all of the lithium halide solutions and alkali fluoride solutions in the frozen state. The distinct differences between the spectra of salt tablets and the frozen solutions indicate hydrate formation. This is also consistent with the previous report,[44] where these lithium and fluoride salts do form hydrates. These results reveal that ions Li^+ and F^- also play substantial roles in salt hydrate formation.

Finally, we studied the effects of the cooling rate and concentration on the formation of salt hydrates. To investigate the effects of the cooling rate on the formation of hydrates, we monitored the changes in terahertz spectra of a fast-frozen NaCl aqueous sample during warm up. The fast-frozen sample was prepared by soaking it into liquid nitrogen directly, and the temperature dropped from room temperature to 80 K within 2 min. The measured spectra are presented in Figure S1a, and for comparison, the spectra of a 1 mol/L NaCl aqueous solution during slow cooling is also inserted into Figure S1b. There is no absorption peak in fast cooling at 80 K due to the formation of the amorphous hydrate while the temperature increases up to 110 K, producing absorption peaks at about 1.6, 2.4, and 3.3 THz, and up 110 K due to the transformation of hydrate from amorphous to crystal. These peaks are generally consistent with slower cooling and are slightly shifted due to the temperature change. Although, freezing rate has certain effects on the formation of salt hydrate, the obtained salt hydrates are the same in slow and fast cooling processes. In our recent results, the terahertz spectra of NaCl solutions with different concentrations at 223 K were recorded.[35] At lower concentrations of 0.1-0.3 mol/L, the peak is invisible due to the detection limit of the terahertz detector. When the concentration is larger than 1.0 mol/L, we could see clearly the terahertz absorption peaks at 1.60, 2.43, and 3.34 THz, indicating the formation of the NaCl hydrate. Thus, there is no obvious effect of concentration on the formation of hydrates in our study.

Thus far, in terms of our terahertz measurements, the ability of 20 alkali halide solutions to form hydrates in the frozen state has been is summarized in Table 1. The numbers in Table 1 indicate the absorption peaks of the alkali halide solutions in the frozen states, the numbers in parentheses refer to the absorption peaks of the nonhydrate salt tablets, and the stars (★) in unit cells indicate the salts that can form hydrates. Most notably, the data in Table 1 clearly show that Na^+, Li^+, and F^- ions play key roles in salt hydrate formation, and all lithium halides, sodium halides, and alkali fluorides are able to form hydrates upon cooling their aqueous solutions except for LiF due to its poor water solubility. However, the nine other salts cannot form hydrates during the freezing process. Our observations here are also consistent with those reported previously using IR spectroscopy.[24]

The key factor in determining whether a salt could form hydrates is the ion-water binding energy. The potential energy of the interaction between the full charge of an ion and the two partial charges of a water molecules is $Ep \propto (-|z|\mu)/r^2$, where z is the charge number of the ion, μ is the electric dipole moment of the water molecule, and r is the distance between the ion and the dipole, which is larger for a larger ion radius.[45] Thus, it is obvious that the binding energy of the ions is closely related to the ionic radius. The ionic radii are: Li^+ (76 pm) <Na^+ (102 pm) <F^- (133 pm) <K^+ (138 pm) <Rb^+ (152 pm) <Cs^+ (167 pm) <Cl^- (181 pm) <Br^- (196 pm) <I^- (220 pm).[45] For the same amount of charge, the smaller ion radius corresponds to a stronger binding energy of ion-water. The first binding energies of Li^+, Na^+ and F^- ions to water molecules are 34, 24 and 23.3 kcal/mol, respectively.[46] The binding energies of these ions are stronger than the total binding energy of 22.2 kcal/mol for the four saturated hydrogen bonds of each H_2O in Ih ice.[47] Thus, even at the eutectic temperature where these ions are recombined with other oppositely charged ions, the strongly

Table 1. Terahertz Absorption Peaks of Alkali Halide Solutions in the Frozen States.

	F^-	Cl^-	Br^-	I^-
Li^+	LiF (slightly soluble in water)	LiCl 2.10, 2.75 ★	LiBr 1.60, 2.28, 2.59, 2.91, 3.41 ★	LiI 3.16 ★
Na^+	NaF 3.30 ★	NaCl 1.60, 2.43, 3.34 ★	NaBr 2.11 ★	NaI 1.25, 1.68 ★
K^+	KF 1.61, 2.29, 2.53, 2.85 ★	KCl	KBr	KI 3.13 (3.17)
Rb^+	RbF 0.75, 1.14, 1.98, 2.56 ★	RbCl	RbBr 2.69 (2.75)	RbI 2.30 (2.31)
Cs^+	CsF 1.28, 2.11, 2.93 ★	CsCl 3.07 (3.14)	CsBr 2.27, 2.71 (2.24)	CsI 1.90, 2.25 (1.90)

bonded water molecules remain and are complementarily filled into their lattice vacancies to make the system the most stable (to minimize the Gibbs free energy of the system), and thereby form a salt hydrate. For example, for the NaCl solution, the binding energy of Na^+ is high enough to interact with the hydrating water molecules to develop many micro $NaCl{\cdot}2H_2O$ crystals.[48] However, for K^+, Rb^+, Cs^+, Cl^-, Br^- and I^- ions, the first ion-water binding energies are 17.9, 15.9, 13.7, 13.1, 12.6 and 10.6 kcal/mol, respectively. These binding energies are smaller than the binding energy of ice.[47] As a result, these ions are extruded out of the hydrogen bond networks and tend to form many micro nonhydrated salt crystals.

In conclusion, the ability of 20 alkali halide solutions to form hydrates in the frozen state has been studied by terahertz time-domain spectroscopy. The distinct change in the terahertz spectrum with the emergence of discrete peaks of the salt solutions in the frozen states has been demonstrated to provide a direct and visible indication of salt hydrate formation. The study revealed that alkali metal cations Na^+ and Li^+ and anion F^- have substantial effects on the salt hydrate formation, which can be attributed to the higher first binding energies of these three ions with water, and they benefit the hydrate-formation process. These observations would therefore establish a simple and conceivable correlation between the terahertz signatures and the salt hydrate formation. Given the extraordinary sensitivity of terahertz spectroscopy, it is believed that such a technique could provide more possibilities for investigations of other hydrate formation systems with different solvents or solutes.

■ ASSOCIATED CONTENT

Supporting Information

■ AUTHOR INFORMATION

Corresponding Authors

*lyliuma@tju.edu.cn
*zhaohongwei@sinap.ac.cn
*jiaghan@tju.edu.cn

Notes

The authors declare no competing financial interest.

■ ACKNOWLEDGMENTS

This work was supported by the National Key Research and Development Program of China (grant no. 2017YFA0701004), the National Science Foundation of China (grant nos. 61875150, 61935015, and 61705163), the Tianjin Municipal Fund for Distinguished Young Scholars (18JCJQJC45600), and the National Defense Science and Technology Innovation Special Zone.

■ REFERENCES

(1) Keys, J. R.; Williams, K. Origin of crystalline, cold desert salts in the McMurdo region, Antarctica, *Geochim. Cosmochim. Acta* **1981**, 45, 2299-2309.

(2) Cullen, D.; Baker, I. The chemistry of grain boundaries in Greenland ice, *J. Glaciol.* **2000**, 46, 703-706.

(3) Ward, M. K.; Pollard, W. H. A hydrohalite spring deposit in the Canadian high Arctic: A potential Mars analogue, *Earth Planet. Sci. Lett.* **2018**, 504, 126-138.

(4) Vaniman, D. T.; Bish, D. L.; Chipera, S. J.; Fialips, C. I.; William Carey, J.; Feldman, W. C. Magnesium sulphate salts and the history of water on Mars, *Nature* **2004**, 431, 663-665.

(5) Cleeves, L. I.; Bergin, E. A.; Alexander, C. M. O. D.; Du, F.; Graninger, D.; Öberg, K. I.; Harries, T. J. The ancient heritage of water ice in the solar system, *Science* **2014**, 345, 1590-1593.

(6) Davila, A. F.; Duport, L. G.; Melchiorri, R.; Jänchen, J.; Valea, S.; de los Rios, A.; Fairén, A. G.; Möhlmann, D.; McKay, C. P.; Ascaso, C.; Wierzchos, J. Hygroscopic salts and the potential for life on Mars, *Astrobiology* **2010**, 10, 617-628.

(7) Wise, M. E.; Baustian, K. J.; Koop, T.; Freedman, M. A.; Jensen, E. J.; Tolbert, M. A. Depositional ice nucleation onto crystalline hydrated NaCl particles: a new mechanism for ice formation in the troposphere, *Atmos. Chem. Phys.* **2012,** 12, 1121-1134.

(8) Abbatt, J. P. D.; Benz, S.; Cziczo, D. J.; Kanji, Z.; Lohmann, U.; Möhler, O. Solid ammonium sulfate aerosols as Ice nuclei: A pathway for cirrus cloud formation, *Science* **2006**, 313, 1770-1773.

(9) Mazur, P. Freezing of living cells: mechanisms and implications, *Am. J. Physiol-Cell Ph.* **1984**, 247, C125-C142.

(10) Okotrub, K. A.; Surovtsev, N. V. Raman scattering evidence of hydrohalite formation on frozen yeast cells, *Cryobiology* **2013**, 66, 47-51.

(11) Kreiner-Møller, A.; Stracke, F.; Zimmermann, H. Hydrohalite spatial distribution in frozen cell cultures measured using confocal Raman microscopy, *Cryobiology* **2014**, 69, 41-47.

(12) Bowers, G. M.; Singer, J. W.; Bish, D. L.; Kirkpatrick, R. J. Alkali metal and H_2O dynamics at the smectite/water interface, *J. Phys. Chem. C* **2011**, 115, 23395-23407.

(13) Nour, S.; Widdifield, C. M.; Kobera, L.; Burgess, K. M. N.; Errulat, D.; Terskikh, V. V.; Bryce, D. L. Oxygen-17 NMR spectroscopy of water molecules in solid hydrates, *Can. J. Chem.* **2016**, 94, 189-197.

(14) Klewe, B.; Pedersen, B. The crystal structure of sodium chloride dihydrate, *Acta Crystallogr., Sect. B: Struct. Cryst. Chem.* **1974**, 30, 2363-2371.

(15) Reddy, U. V.; Bowers, G. M.; Loganathan, N.; Bowden, M.; Yazaydin, A. O.; Kirkpatrick, R. J. Water structure and dynamics in smectites: X-ray diffraction and ^2H NMR spectroscopy of Mg-, Ca-, Sr-, Na-, Cs-, and Pb-hectorite, *J. Phys. Chem. C* **2016**, 120, 8863-8876.

(16) Hennings, E.; Schmidt, H.; Voigt, W. Crystal structures of hydrates of simple inorganic salts. I. Water-rich magnesium halide hydrates $MgCl_2{\cdot}8H_2O$, $MgCl_2{\cdot}12H_2O$, $MgBr_2{\cdot}6H_2O$, $MgBr_2{\cdot}9H_2O$, $MgI_2{\cdot}8H_2O$ and $MgI_2{\cdot}9H_2O$, *Acta Crystallogr., Sect. C: Cryst. Struct. Commun.* **2013**, 69, 1292-1300.

(17) Hennings, E.; Schmidt, H.; Voigt, W. Crystal structures of hydrates of simple inorganic salts. II. Water-rich calcium bromide and iodide hydrates: $CaBr_2{\cdot}9H_2O$, $CaI_2{\cdot}8H_2O$, $CaI_2{\cdot}7H_2O$ and $CaI_2{\cdot}6.5H_2O$, *Acta Crystallogr., Sect. C: Struct. Chem.* **2014**, 70, 876-881.

(18) Chiari, G.; Ferraris, G. The water molecule in crystalline hydrates studied by neutron diffraction, *Acta Crystallogr., Sect. B: Struct. Cryst. Chem.* **1982**, 38, 2331-2341.

(19) Lokshin, K. A.; Zhao, Y.; He, D.; Mao, W. L.; Mao, H.-K.; Hemley, R. J.; Lobanov, M. V.; Greenblatt, M. Structure and dynamics of hydrogen molecules in the novel clathrate hydrate by high pressure neutron diffraction, *Phys. Rev. Lett.* **2004**, 93, 125503.

(20) Yamashita, K.; Komatsu, K.; Hattori, T.; Machida, S.; Kagi, H. Crystal structure of a high-pressure phase of magnesium chloride hexahydrate determined by in-situ X-ray and neutron diffraction methods, *Acta Crystallogr., Sect. C: Struct. Chem.* **2019**, 75, 1605-1612.

(21) Bellamy, L. J.; Blandamer, M. J.; Symons, M. C. R.; Waddington, D. Infra-red spectra of salt hydrates. Correlation between the fundamental symmetric and asymmetric stretching frequencies of the water molecules, *Trans. Faraday Soc.* **1971**, 67, 3435-3440.

(22) Lutz, H. D. *In Solid Materials*; Springer Berlin, **1988**, p 97-125.

(23) Pandelov, S.; Pilles, B. M.; Werhahn, J. C.; Iglev, H. Time-resolved dynamics of the OH stretching vibration in aqueous NaCl hydrate, *J. Phys. Chem. A* **2009**, 113, 10184-10188.

(24) Pandelov, S.; Werhahn, J. C.; Pilles, B. M.; Xantheas, S. S.; Iglev, H. An empirical correlation between the enthalpy of solution of aqueous salts and their ability to form hydrates, *J. Phys. Chem. A* **2010**, 114, 10454-10457.

(25) Werhahn, J. C.; Pandelov, S.; Xantheas, S. S.; Iglev, H. Dynamics of weak, bifurcated, and strong hydrogen bonds in lithium nitrate trihydrate, *J. Phys. Chem. Lett.* **2011**, 2, 1633-1638.

(26) Wagner, R.; Möhler, O.; Schnaiter, M. Infrared optical constants of crystalline sodium chloride dihydrate: application to study the crystallization of aqueous sodium chloride solution droplets at low temperatures, *J. Phys. Chem. A* **2012**, 116, 8557-8571.

(27) Werhahn, J. C.; Xantheas, S. S.; Iglev, H. *Research in Optical Sciences*; Optical Society of America: Berlin, **2012**, p JT2A.45.

(28) Hutzler, D.; Brunner, C.; Petkov, P. S.; Heine, T.; Fischer, S. F.; Riedle, E.; Kienberger, R.; Iglev, H. Dynamics of the OH stretching mode in crystalline $Ba(ClO_4)_2 \cdot 3H_2O$, *J. Chem. Phys.* **2018**, 148, 054307.

(29) Maréchal, Y. *The Hydrogen Bond and the Water Molecule: the Physics and Chemistry of Water, Aqueous and Bio Media*, Elsevier, Amsterdam, **2007**. (Chapter 10)

(30) Baxter, J. B.; Guglietta, G. W. Terahertz Spectroscopy, *Anal. Chem.* **2011**, 83, 4342-4368.

(31) McIntosh, A. I.; Yang, B.; Goldup, S. M.; Watkinson, M.; Donnan, R. S. Terahertz spectroscopy: a powerful new tool for the chemical sciences?, *Chem. Soc. Rev.* **2012**, 41, 2072-2082.

(32) Ueno, Y.; Ajito, K. Analytical terahertz spectroscopy, *Anal. Sci.* **2008**, 24, 185-192.

(33) Takahashi, M. Terahertz vibrations and hydrogen-bonded networks in crystals, *Crystals* **2014**, 4, 74-103.

(34) Ajito, K.; Ueno, Y.; Kim, J.-Y.; Sumikama, T. Capturing the freeze-drying dynamics of NaCl nanoparticles using THz spectroscopy, *J. Am. Chem. Soc.* **2018**, 140, 13793-13797.

(35) Chen, L.; Ren, G.; Liu, L.; Guo, P.; Wang, E.; Zhu, Z.; Yang, J.; Shen, J.; Zhang, Z.; Zhou, L.; Zhang, J.; Yang, B.; Zhang, W.; Gao, Y.; Zhao, H. Han. J. Probing NaCl hydrate formation from aqueous solutions by Terahertz Time-Domain Spectroscopy, *Phys. Chem. Chem. Phys.* DOI: 10.1039/d0cp01571g.

(36) Shen, Y. C.; Upadhya, P. C.; Linfield, E. H.; Davies, A. G. Temperature-dependent low-frequency vibrational spectra of purine and adenine, *Appl. Phys. Lett.* **2003**, 82, 2350-2352.

(37) Zeitler, J. A.; Newnham, D. A.; Taday, P. F.; Strachan, C. J.; Pepper, M.; Gordon, K. C.; Rades, T. Temperature dependent terahertz pulsed spectroscopy of carbamazepine, *Thermochim. Acta* **2005**, 436, 71-77.

(38) Brüesch P. *Phonons: Theory and Experiments II—Experiments and Interpretation of Experimental Results* Springer, Berlin, **1986**.

(39) Van Meerssche, P. M.; Dereppe, J. M.; Lono P. W. *Structure protonique de* $NaBr_2 \cdot H_2O$. Bulletin de la Societe Francaise de Mineralogie et de Cristallographie **1962**, 85, 290-292.

(40) Parker, V. B. *National Standard Reference Data Series*; National Bureau of Standards 2, **1965**.

(41) Kim, B. H.; Heo, J.; Kim, S.; Reboul, C. F.; Chun, H.; Kang, D.; Bae, H.; Hyun, H.; Lim, J.; Lee, H.; Han, B.; Hyeon, T.; Alivisatos, A. P.; Ercius, P.; Elmlund, H.; Park, J. Critical differences in 3D atomic structure of individual ligand-protected nanocrystals in solution. *Science* **2020**, 368(6486), 60-67.

(42) Zhang, W.; Qin, X.; Zhang, L. Lattice distortion of nanoscale silver particles. *Chin. Sci. Bull.* **1998**, 43, 201-204.

(43) Ghosh, A. K.; Manna, A. Lattice distortion due to isovalent impurities in ionic crystals. *J. Phys. Chem. Solids* **1982** 43(4), 415-416.

(44) Sohr, J.; Schmidt, H.; Voigt, W. Higher hydrates of lithium chloride, lithium bromide and lithium iodide. *Acta Crystallogr., Sect. C: Struct. Chem.* **2018**, 74, 194-202.

(45) Peter Atkins, L. J. *Chemical Principles The Quest for Insight* Freeman, New York, **2009**, p172-173.

(46) Keesee, R. G.; Castleman, A. W. Thermocemical data on gas-phase ion-molecule association and clustering reactions, *J. Phys. Chem. Ref. Data* **1986**, 15, 1011-1071.

(47) Son, L.; Rusakov, G. Liquid-liquid phase transitions: analytical approaches, *J. Phys.: Condens. Matter* **2008**, 20, 114108 (1).

(48) Tsironi, I.; Schlesinger, D.; Spah, A.; Eriksson, L.; Segad, M.; Perakis, F. Brine rejection and hydrate formation upon freezing of NaCl aqueous solutions, *Phys. Chem. Chem. Phys.* **2020**, 22, 7625-7632.